

EN 1991-2 traffic loads design charts for closed rib orthotropic deck plate based on Pelikan-Esslinger method

Andjelko Vlastic*, Jure Radic and Zlatko Savor

Faculty of Civil Engineering, University of Zagreb, Kaciceva 26, 10000 Zagreb, Croatia

(Received November 7, 2008, Accepted February 5, 2009)

Abstract. Charts for the bending moments in the closed rib orthotropic deck plate are derived, based on the method originally introduced by Pelikan and Esslinger. New charts are done for EN 1991-2 traffic load distribution schemes. The governing Huber plate equation is solved utilizing Fourier series for various bridge deck plate boundary conditions. Bending moments are given as a function of deck plate rigidities and span length between cross beams. Old diagrams according to DIN 1072, the new ones according to EN 1991-2 and FE analyses results are compared. For typical bridge orthotropic deck plates, it can be concluded that the new EN 1991-2 traffic loads produce larger mid-span bending moments when two lane schemes are used, then those of DIN 1072. For support moments, DIN 1072 gives larger values for any number of lanes, especially under span lengths of 5m. The relevant differences are up to 25%.

Keywords : bridge; orthotropic deck plate; closed rib; traffic load; bending moments.

1. Introduction

In the design of the closed rib orthotropic plate, local effects of vehicle axle loads contribute to the global stress state and have to be accounted for. A widely spread calculation method relies on the available design charts to determine directly section moments. These charts were first introduced by W. Pelikan and M. Esslinger in 1957 (Pelikan and Esslinger 1957) and later expanded by H. U. Gauger and J. Oxfort in 1983 (Gauger and Oxfort 1983). They were specifically developed for calculation of bending moments due to the DIN 1072 traffic load distribution schemes, the former one for one heavy vehicle traffic lane scheme, and the latter one for two heavy vehicle lanes scheme. Until recently, these charts were largely used in design due to their simplicity and accuracy. With implementation of the new Eurocode norm, new traffic load schemes were introduced, which are very different from the DIN 1072, in reference to axle number and load values. Finite element models of these plates can often be too large and complex for practical purposes. Therefore, authors' aim was to provide charts similar to those of Pelikan-Esslinger and Gauger-Oxfort, so that the well known calculation method of closed rib orthotropic deck plate can be used again with the EN 1991-2 schemes (EN 1991-2 2003). To achieve this the Huber equation was solved based on the Pelikan-Esslinger method (Pelikan and Esslinger 1957). Computer algorithm was written to find solutions for all possible closed rib orthotropic deck plate parameters, and the data was stored in an extensive data base from which the new charts were drawn.

* Corresponding Author, Email: vlastic@grad.hr

The Pelikan-Esslinger method is divided into two stages of calculation. First, according to the relevant parameter H/D_y , bending moments in the rigidly supported deck are determined from charts. Secondly, relief moments are determined as the consequence of the elastic flexibility of the cross beams. These moments are defined as the product of the traffic load distribution factors Q_x/Q_0 (which are dependent on the plate width b), load intensity Q_0 , plate span s , and the dimensionless bending moment factors depending on the relief factor γ . Finally, the moments from the two stages are summed, giving the real moment.

2.2 Traffic load according to EN 1991-2

New Eurocode traffic load trains used to derive bending moments diagrams are shown in Fig. 2 (EN 1991-2, 2003). Each of the lanes, q_1 and q_2 are also loaded with the continuous loading, with $q_1 = 9 \text{ kN/m}^2$, and $q_2 = 2.5 \text{ kN/m}^2$. The rest of the bridge is loaded with $q_2 = 2.5 \text{ kN/m}^2$. Depending on the width of the bridge, traffic scheme with only one ($< 6\text{m}$ roadway width) or two ($\geq 6\text{m}$) traffic lanes is selected. The reduction factor α_Q is set to 0.8 according to DIN-Fachbericht 101.

3. Equation solution

3.1 Form of the solution

The orthotropic plate is represented by the general form of the Huber equation (Troitsky 1967):

$$D_x \frac{\partial^4 w}{\partial x^4} + 2H \frac{\partial^4 w}{\partial x^2 \partial y^2} + D_y \frac{\partial^4 w}{\partial y^4} = p(x, y) \tag{4}$$

where D_x and D_y are plate flexural rigidities in transverse and longitudinal direction, w is the plate point displacement, and p is the vertical load.

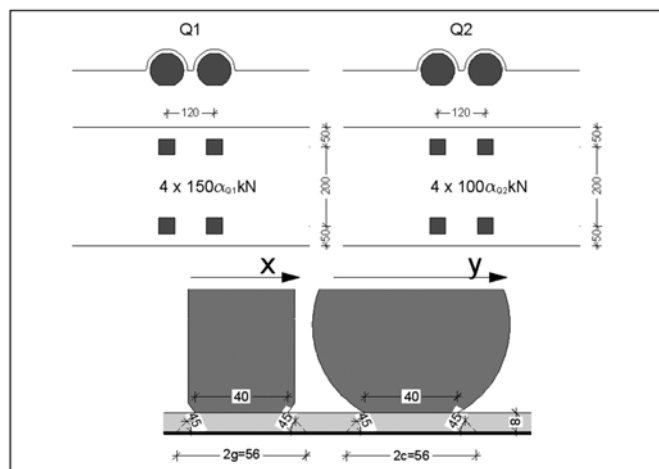


Fig. 2 Traffic load according to EN 1991-2 (Load model 1)

Given that the transverse rigidity is much smaller than the longitudinal, the expression can be written:

$$2H \frac{\partial^4 w}{\partial x^2 \partial y^2} + D_y \frac{\partial^4 w}{\partial y^4} = p(x, y) \tag{5}$$

The solution to this equation can be found as:

$$w = w_h + w_p \tag{6}$$

where w_h is the solution to the homogenous equation

$$2H \frac{\partial^4 w}{\partial x^2 \partial y^2} + D_y \frac{\partial^4 w}{\partial y^4} = 0$$

$$w_h = \sum_{n=1}^{\infty} (C_{1n} \sinh \alpha_n y + C_{2n} \cosh \alpha_n y + C_{3n} \alpha_n y + C_{4n}) \sin \frac{n\pi x}{b} \tag{7}$$

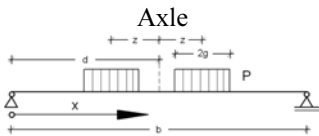
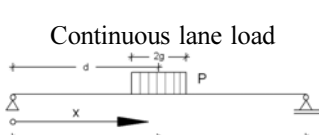
$$\alpha_n = \frac{n\pi}{b} \sqrt{\frac{2H}{D_y}} \tag{8}$$

and the w_p is the particular solution:

$$w_p = \frac{1}{D_x} \sum_{n=1}^{\infty} \left(\frac{b}{n\pi}\right)^4 p(x) \tag{9}$$

In order for the equation to be solved, both of the solutions must be expressed with Fourier series. Necessary transformations to the axle load $p(x)$ from the Fig. 2 are made in the Table 1 and shown in

Table 1 Traffic load represented in Fourier series

| Load distribution | Fourier series | Simplification for given conditions |
|---|---|--|
|  | $\frac{Q_{nx}}{Q_0} = \frac{8}{n\pi} \cos \frac{n\pi z}{b} \sin \frac{n\pi g}{b} \sin \frac{n\pi d}{b} \sin \frac{n\pi x}{b}$ | $x = b/2 - z$ (analyzed point under the wheel) $\frac{Q_{nx}}{Q_0} = \frac{8}{n\pi} \cos^2 \frac{n\pi z}{b} \sin \frac{n\pi g}{b}$ |
|  | $\frac{Q_{nx}}{Q_0} = \frac{4}{n\pi} \sin \frac{n\pi g}{b} \sin \frac{n\pi d}{b} \sin \frac{n\pi x}{b}$ | $d = b/2$ (load is in the middle) $\frac{Q_{nx}}{Q_0} = \frac{4}{n\pi} \sin \frac{n\pi g}{b} \sin \frac{\pi n}{2} \sin \frac{n\pi x}{b}$ |
| | | $x = b/2$ (analyzed point is in the middle) $\frac{Q_{nx}}{Q_0} = \frac{4}{n\pi} \sin \frac{n\pi g}{b} \sin \frac{\pi n}{2}$ |

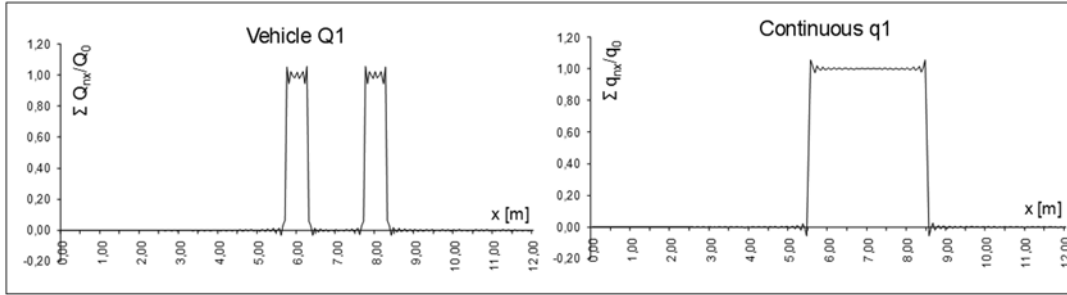


Fig. 3 EN 1991-2 traffic load expressed by Fourier series

Fig. 3, using 309 members. Convergence was already achieved with 110 members.

Using the affinity, because both loads and deformations are expressed with sinusoidal functions, two dimensional plate problem can be transformed into one dimensional. Therefore, instead of influence surfaces, influence lines may be used.

3.2 Influence lines and bending moments for rigid support deck

Moments for rigid support deck are obtained using the expression (Troitsky 1967, Horvatic 1977):

$$M = Q_0 s \sum_{n=1}^{\infty} \frac{Q_{nx} \eta_n}{Q_0 s} \quad (10)$$

where η_n/s is influence line for the unit span deck plate, and $Q_0 = P/2g$, P being the wheel load. Assuming a hinge in the location for which an influence line is sought, and allowing a unit rotation $1 \cdot \sin(n\pi x/b)$ in that hinge, a deflection line is obtained. Ordinates of this deflection line are by definition the ordinates of influence line. Integration constants C_n for solution of Eq. (7) are found by applying the boundary conditions and conditions of continuity above supports. Also, the three moment equations for the support moments are used.

Influence lines have to be calculated for the midspan moment and support moment separately. For a midspan moment influence line is, as follows (Troitsky 1967, Horvatic 1977):

$$\frac{\eta_{cn}}{s} = \frac{1}{2\alpha} \frac{1}{\cosh \frac{\alpha s}{2}} \sinh \alpha y + \frac{M_0^*}{s} \left(\tanh \frac{\alpha s}{2} \sinh \alpha y - \cosh \alpha y + 1 \right) \quad (11)$$

where:

$$\frac{M_0^*}{s} = \frac{R}{1-R} \frac{1}{2\alpha^* \cosh \frac{\alpha s}{2}} \quad (12)$$

$$R = -k + \sqrt{k^2 - 1}; \quad k = \frac{\alpha s \coth \alpha s - 1}{\alpha^*}; \quad \alpha^* = 1 - \frac{\alpha s}{\sinh \alpha s}$$

This form of influence line is valid only for the loaded span. Because the EN 1991-2 vehicle is always in this span for the maximum mid-span moment, it suffices to use this form.

For a support moment the influence line is expressed, as (Troitsky 1967, Horvatic 1977):

$$\frac{\eta_{sn}}{s} = \frac{M_0^*}{s} \left(\frac{\cosh \alpha s - R}{\sinh \alpha s} \sinh \alpha y - \cosh \alpha y + \frac{R-1}{\alpha s} \alpha y + 1 \right) \quad (13)$$

$$M_0^* = \frac{R}{1 - R^2} \frac{s}{\alpha^*} \quad (14)$$

If this expression is to be used in spans other than the ones bordering the support for which the moment is to be found, it is necessary to multiply it by a reduction factor R_m (m is the integer number of the support, where $m = 0$ is the starting support).

In all these influence line expressions, y is the position of the axle from support. It is not necessary to perform an integration of the influence line under the wheel area; it is enough to take its ordinate value in the axle axis. This is true in all but one case, for the mid-span moment under the direct wheel load. There the influence line needs to be integrated or otherwise it will produce too large a moment (Pelikan and Esslinger 1957):

$$2 \int_{\frac{s}{2}-c}^{\frac{s}{2}} \frac{\eta_{cn}}{s} = \sum \left[\frac{1}{2 \alpha_n s \alpha_n c} \left[1 - \frac{\cosh \left[\alpha_n \left(\frac{s}{2} - c \right) \right]}{\cosh \frac{\alpha_n s}{2}} \right] + \frac{M_0^*}{s} \left[1 - \frac{\sinh \alpha_n c}{\alpha_n c \cosh \frac{\alpha_n s}{2}} \right] \right] \quad (15)$$

Also, the moment from the continuous traffic loading is to be accounted for by integration of the influence line in the spans where this loading is applied. In case of mid-span moment this integration gives the expression:

$$M_{00}^q = qs^2 \left[\frac{\cosh \alpha \frac{s}{2} - 1}{(\alpha s)^2 \cosh \alpha \frac{s}{2}} + \frac{M_0^*}{s} \left(1 - \frac{2}{\alpha s} \tanh \alpha \frac{s}{2} \right) \right] \quad (16)$$

In case of support moment, integration gives the expression:

$$M_{01}^q = \frac{qs^2}{2} \frac{R}{\alpha^* (1-R)} \left[1 - \frac{2}{\alpha s} \tanh \frac{\alpha s}{2} \right] \quad (17)$$

The q load refers to the main traffic lane continuous loading, as all others can be neglected.

When all influence lines are calculated, the position of the vehicle that gives the most unfavorable moment has to be determined. This was achieved by employing a computer algorithm that sums the

two ordinates distanced 1.2m (axle distance) from each other. When the maximum sum is found, a moment is calculated and stored. When two lanes are taken into account, the influence line for the second vehicle is somewhat different. The difference is best represented by section cuts through the influence surface, as shown in Fig. 4.

Intersected curves from planes a. and b. give influence lines similar to those of the main and adjacent traffic lane. Because they are not affine, they do not necessarily have the same position of tandem vehicles for maximum moment as the position when only main lane vehicle is present. In Figs. 5 and 6 the influence lines for support and mid-span moments can be seen, together with relevant vehicle axles positions for both, the Q1 vehicle only, and for the tandem vehicles. Influence lines are given for plate parameters $s = 4m$ and $H/D_y = 0.0246$.

For the example of mid-span influence line (Fig. 6), the position of alone Q1 vehicle and tandem vehicles for maximum moments is the same. In Fig. 5 the position of the vehicle that gives the maximum hogging bending moment at support is in the span. This is not always the case. With the shorter spans, and larger H/D_y ratios, the relevant vehicle position for maximum hogging moment will be when the vehicle is positioned just above the support, with one axle left, and the other right of the support. The ranges of spans and H/D_y ratios, where one or the other position is relevant, are shown in Fig. 7.

In order to build a database for charts of bending moments for all span lengths s and H/D_y ratios that are considered, an algorithm was made which loops the variable s from 3m to 6m in 0.25m steps, and the

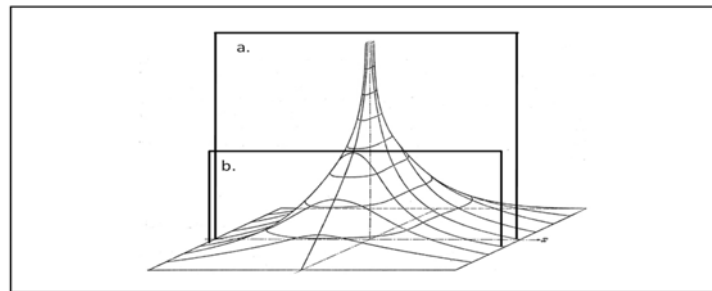


Fig. 4 Surface area sections

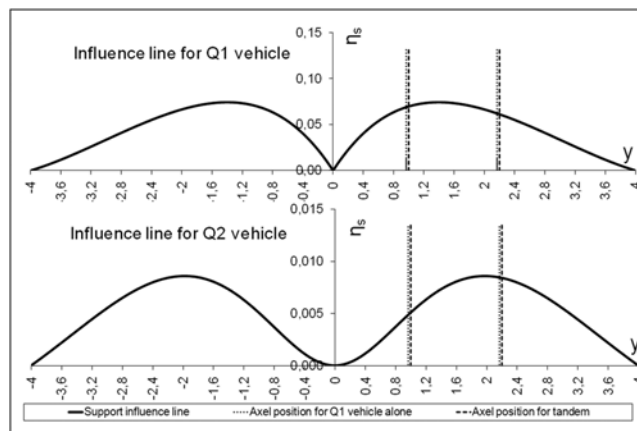


Fig. 5 Support moment influence lines

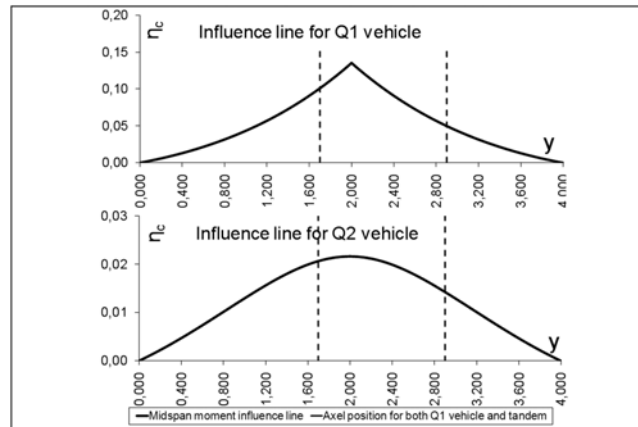


Fig. 6 Mid-span moment influence lines

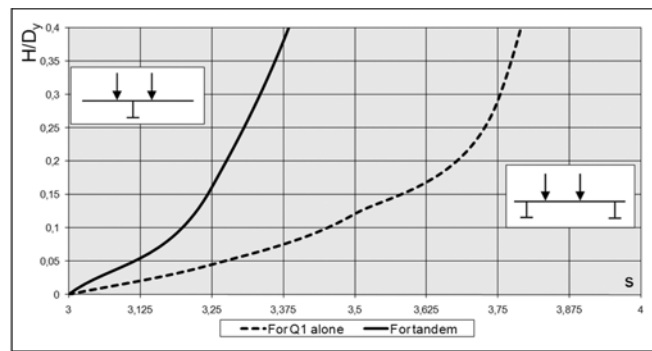


Fig. 7 Relevant axle positions for maximum hogging support moment

variable H/D_y from 0 to 0.3 with the step 0.01. The algorithm automatically sums the moments from the vehicles and the continuous loading, for each of the traffic load schemes - one lane (Q1) and two lanes (Q1+Q2) schemes. Along with the moments, relevant vehicle positions for each span length are also saved, as they will be needed in the second stage for the calculation of relief moments.

Finally, charts for the support and mid-span moments for the one lane scheme are given in the Fig. 8, and for two lanes scheme in the Fig. 9. All these charts are calculated for the deck plate width of 12m, which is more than enough to allow that the longitudinal supports at positions $x = 0$ and $x = b$ do not influence the moments distribution in the middle of a plate, even when the longest span ($s = 6m$) and the smallest H/D_y ratio are analyzed. As in the original Pelikan-Esslinger charts (Pelikan and Esslinger 1957), these charts moments also show the maximum values of moment distribution under the rib that is loaded with the wheel and are given in units [kNm/m]. Conservatively, the total moment that is to be used for design purposes is calculated by multiplying chart moment and the width of one rib: $M_{total} = M_{chart}(a + e)$.

3.3 Effects of elastic supports - relief moments

Moments obtained for the rigidly supported deck, have to be corrected by taking into account the elastic flexibility of the cross beams. Thus the load is transferred to the ribs that are not directly loaded.

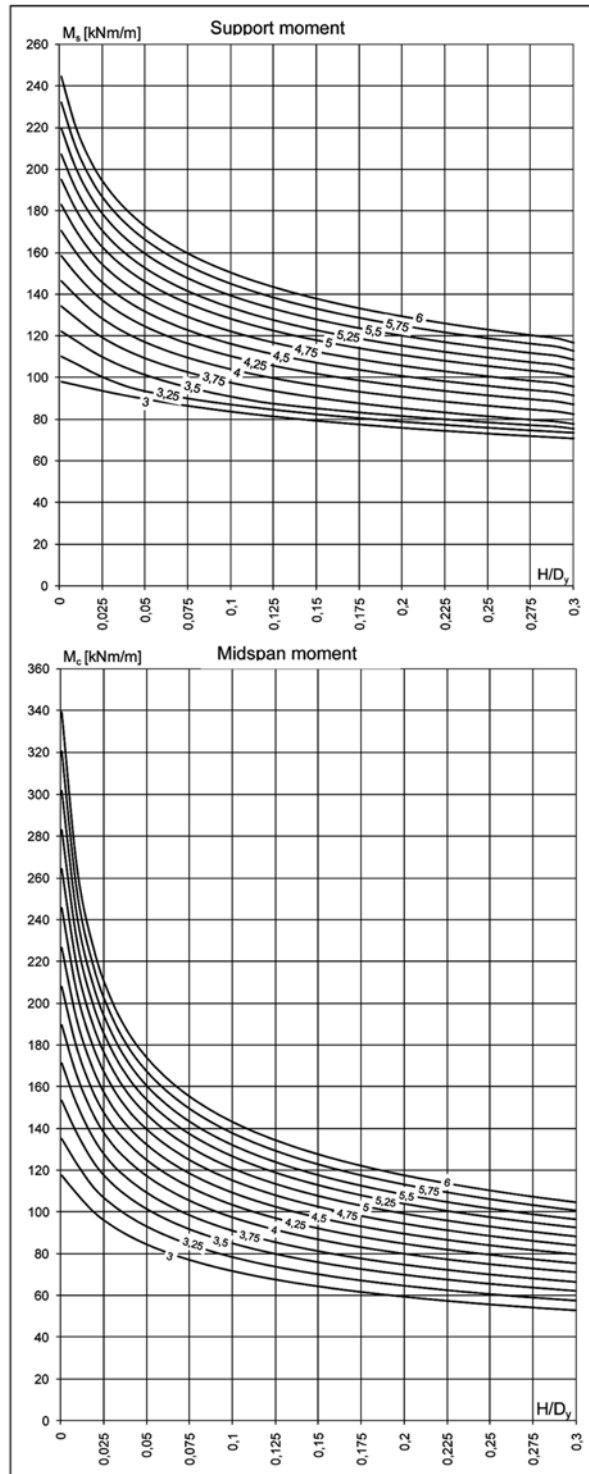


Fig. 8 Bending moments for rigid support deck and one lane traffic load

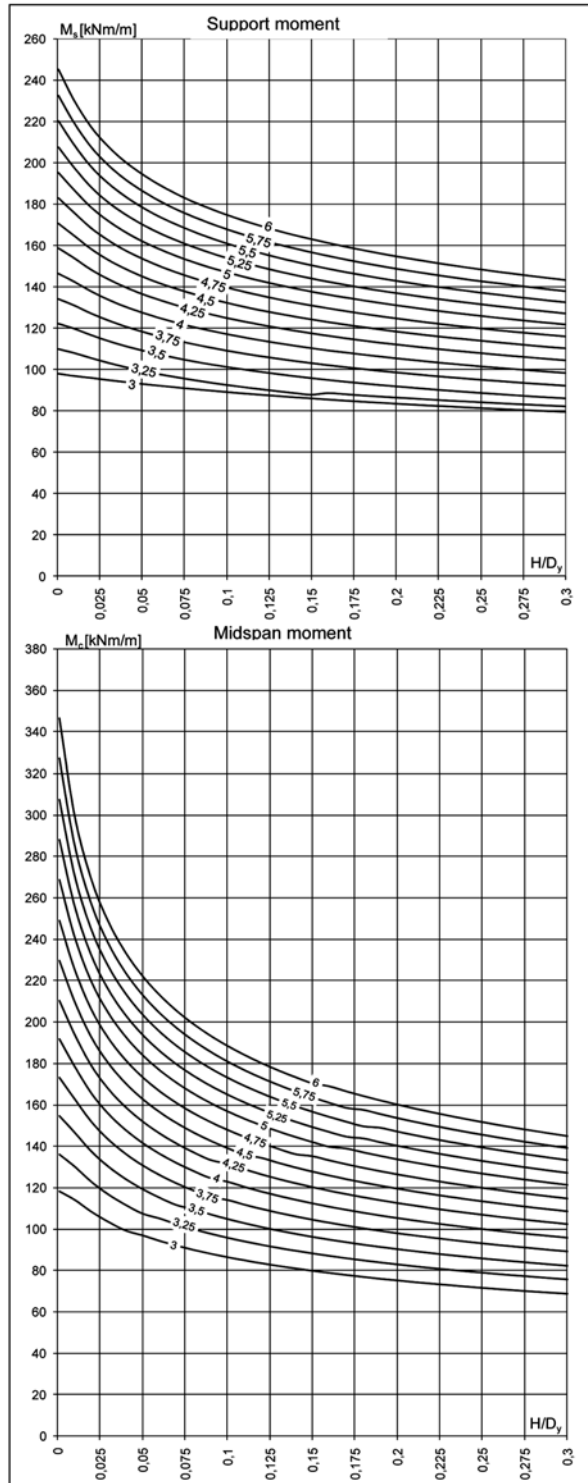


Fig. 9 Bending moments for rigid support deck and two lanes traffic load

Both, transverse and torsion rigidity are neglected, so the plate can be analyzed as an array of parallel bands which act as continuous girders on elastic supports. The reaction of each band on the support is proportional to the deformation of that support. The proportionality factor is defined as the relief factor and is given in the Eq. (3). Because the cross beams are simply supported beams and their deformation is of sinusoidal form, the load also has to be transformed to this form. This is why the axle load $P = 2gQ_0$ can be expressed by using only the first member of the Fourier series from the Table 1. The main problem here is to determine the transverse position of the vehicle(s) that cause(s) the cross beam to deform the most. Another algorithm was made which moves the vehicle(s) from left to right in transverse direction and for each position examines the first Fourier member in a point under the wheel. The largest of them is recorded. In Fig. 10, vehicle positions calculated by algorithm are shown, which are the most relevant for the deck slab width of 7m for both schemes, with one lane and with two lanes. To obtain only one value for vehicles and one for the continuous loading, values from both vehicles and all continuous loadings were summed, by reducing the contributions of loads outside the main lane with a corresponding factor of load intensity ratios.

All this is repeated in a loop encompassing changes of the deck slab width from 3 to 24m (two lanes are possible only for width ≥ 6 m). Diagrams produced from the collected data are shown in Figs. 11 and 12. To calculate the relief moment, reactions on each of the cross beam have to be known. These reactions are a function of the vehicle axles position (Fig. 13a) (Troitsky 1967):

- when the load is in the span 0-1:

$$\frac{K}{P} = 1 - 2.1961\left(\frac{y}{s}\right)^2 + 1.1961\left(\frac{y}{s}\right)^3 \tag{18}$$

- when the load is in other spans:

$$\frac{K}{P} = \left[-0.8038\left(\frac{y}{s}\right) + 1.3923\left(\frac{y}{s}\right)^2 - 0.5885\left(\frac{y}{s}\right)^3 \right] (-0.268)^{m-1} \tag{19}$$

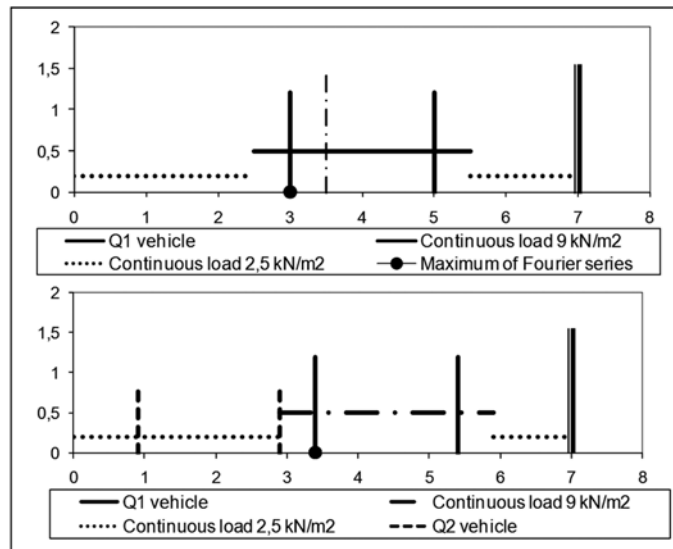


Fig. 10 Finding the relevant vehicle position in deck transverse direction

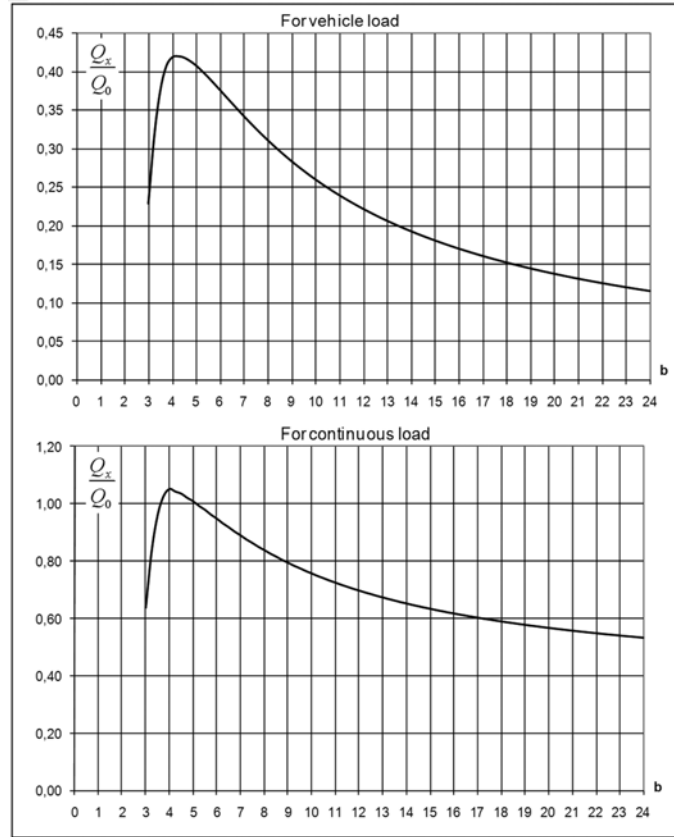


Fig. 11 First Fourier series member for load of one traffic lane

Longitudinal vehicles positions y for each span s and H/D_y ratio are already known from the previous stage of the calculation, so the Eqs. (18) and (19) can be calculated for the unit load and for the each span. For continuous loading, reaction factors are shown in the Fig. 13b (support moment) and Fig. 13c (mid-span moment).

The relief moment expression can be written as:

$$\Delta M = Q_0 s \frac{Q_{1x}}{Q_0} \sum_{m=0}^{\infty} \frac{K_m \bar{\eta}_{im}}{P s} \quad (20)$$

where $\bar{\eta}_{im}/s$ is the ordinate of the influence line for the relief moment above the supports. Again, both, the support relief moment, and the mid-span relief moment have to be calculated. Each of them uses a different influence line, whose values are taken from the Troitsky 1967. They are function of the relief factor γ , as defined in Eq. (3).

The algorithm was written to calculate the following value for each span and each γ :

- in case of vehicle load

$$\sum_{m=0}^{\infty} \frac{K_m \bar{\eta}_{im}}{P s} = \frac{M}{Q_x s} \quad (21)$$

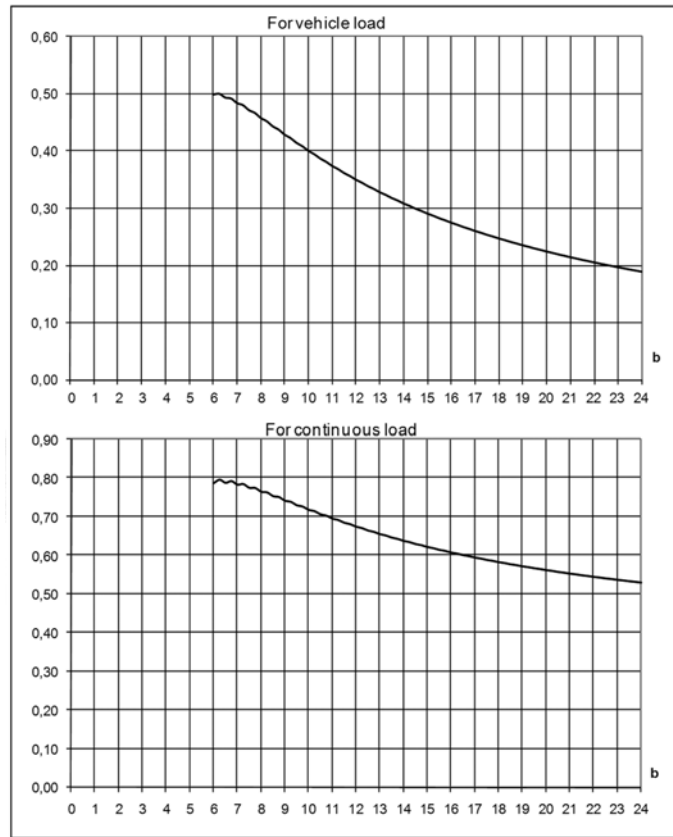


Fig. 12 First Fourier series member for load of two traffic lanes

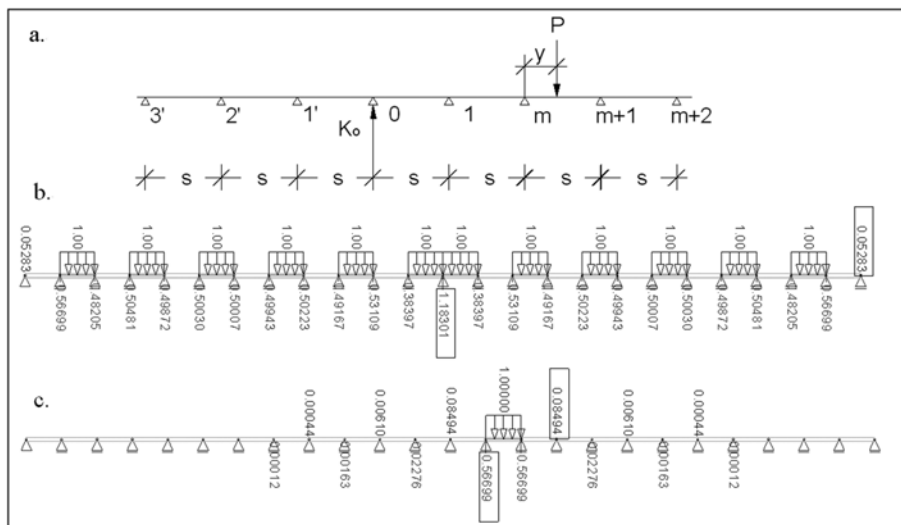


Fig. 13 Reactions on a continuous girder

- in case of continuous loading

$$\sum_{m=0}^{\infty} \frac{K_m \bar{\eta}_{im}}{P^S s} = \frac{M}{Q_x s^2} \tag{22}$$

These are called dimensionless relief bending moments and are given separately for the vehicle loads (Fig. 14) and for the continuous loading (Fig. 15). It is interesting to observe how the relief support moments are much larger for spans of 3 and 3.5m. This is because in these spans, the vehicle that gives the largest support moment is positioned just above the cross beam as shown in Fig. 7. In this case the deflection of the cross beam will be the largest.

For continuous loading, there are two possible load schemes. For the mid-span, and rigid supports, the largest moment will occur when the spans are loaded like a checkerboard, but in this case the deflections of all the cross beams are the same and therefore no relief moments ensue. For the support moment, on the other hand, both possibilities exist, and hence relief moments will ensue. However, it is recommended to use the scheme with all the relevant spans loaded, for it will give the largest moment on the system with rigid supports. True, in this case there is less cross beam deflection, but anyway the deflection is not important because when designing the orthotropic deck plate for maximum hogging moments, the rigid support system is the governing one.

Finally, relief moments are obtained:

- for vehicle load

$$\Delta M = Q_0^{Q_1} s \frac{Q_{1x}}{Q_0} \sum_{m=0}^{\infty} \frac{M}{Q_x s} \tag{23}$$

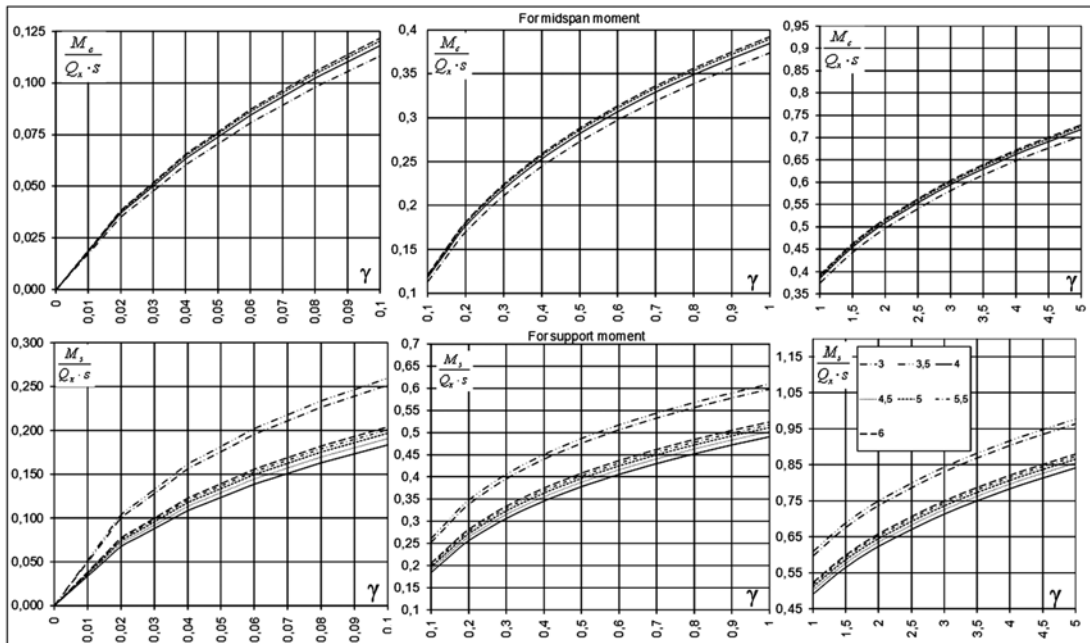


Fig. 14 Dimensionless relief moments for vehicle load

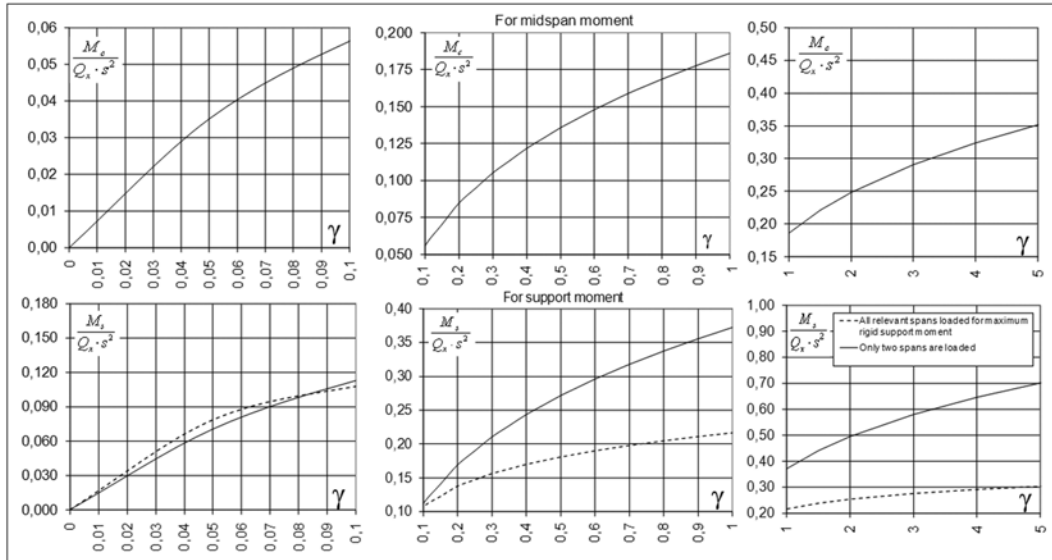


Fig. 15 Dimensionless relief moments for continuous loading

- for continuous loading

$$\Delta M = Q_0^q s^2 \frac{Q_{1x}}{Q_0} \sum_{m=0}^{\infty} \frac{M}{Q_x s^2} \tag{24}$$

where $Q_0^{Q_1} = 120/0.56[kN/m]$, and $Q_0^q = 9[kN/m^2]$.

4. Comparison of analytical and numerical results

Using a finite element software package Sofistik 23, a model was constructed. It consists solely of plane elements that have flexural and torsion rigidity in both plane directions. Two alternatives of the model were made – the one for rigidly supported deck (a), and the other for elastically supported deck (b). Both models are shown in the Fig. 16. FE models were made for two types of orthotropic deck plate (Type 1 and Type 2) and each type for spans of 3, 4, 5 and 6m - altogether 16 models.

All the models were loaded with EN 1991-2 traffic load schemes (EN 1991-2 2003), as well as DIN 1072 schemes. This was done to find a suitable finite element size where the error correlation between the analytical and numerical solutions would be similar for Pelikan-Esslinger (Pelikan and Esslinger 1957) and Gauger-Oxford (Gauger and Oxford 1983) diagrams and for the newly derived EN 1991-2 diagrams. Through extensive model iterations it was observed how results vary depending on the element size, and the most suitable mesh size around supports and in the mid-span was adopted.

A comparison was made between the analytical and numerical results for both types of the orthotropic plate, on rigid supports and on elastic supports, for both DIN 1072 and EN 1991-2 traffic loadings. In Fig. 17 comparison charts are given for Type 1 plate and two traffic lanes load.

By analyzing the comparisons made from all 16 models, the following conclusions can be made:

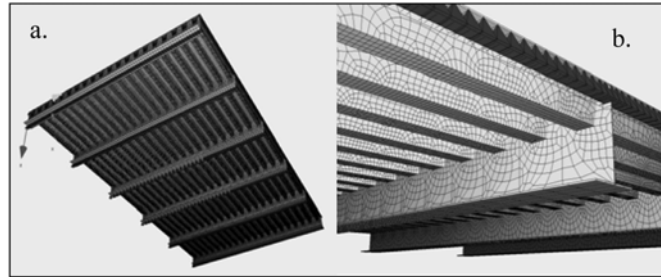


Fig. 16 Closed rib orthotropic deck finite element model

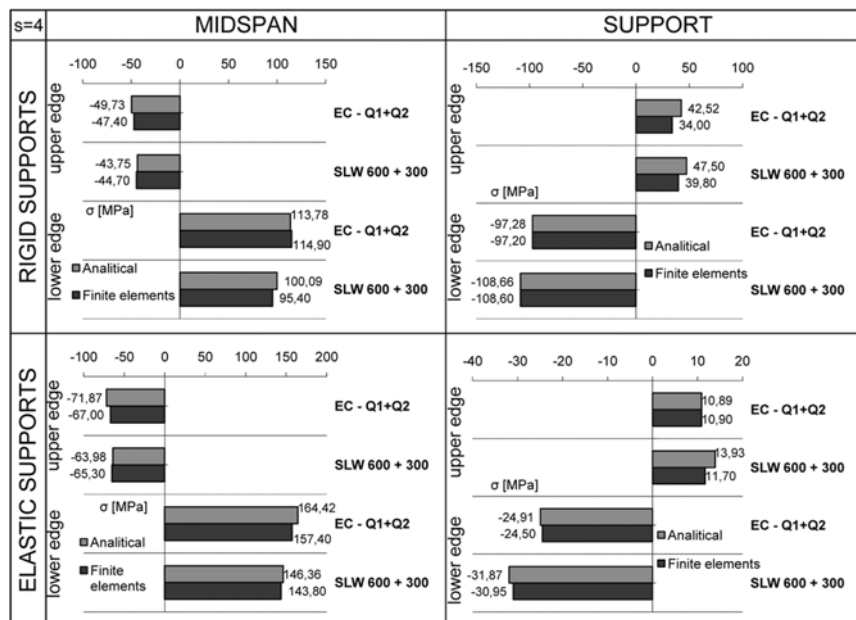


Fig. 17 Comparison charts for EN 1991-2 and DIN 1072 orthotropic deck plate stresses (two lanes)

1. Correlation of errors between DIN 1072 and EN 1991-2 analytical and numerical calculation is the same. This confirms the accuracy of the newly derived diagrams.
2. Analytical calculations are on the safe side, which is to be expected due to their initial assumptions.
3. Error between the analytical and numerical calculation is a consequence of local stresses and is found to be acceptable. The largest error observed is 13.7% with the largest spans of 6m. In more than half the cases the error is less than 3%.

5. Comparison of bending moments according to DIN 1072 and EN 1991-2

5.1 Rigid support deck

A comparison between Pelikan-Esslinger charts (Pelikan and Esslinger 1957) and new charts is

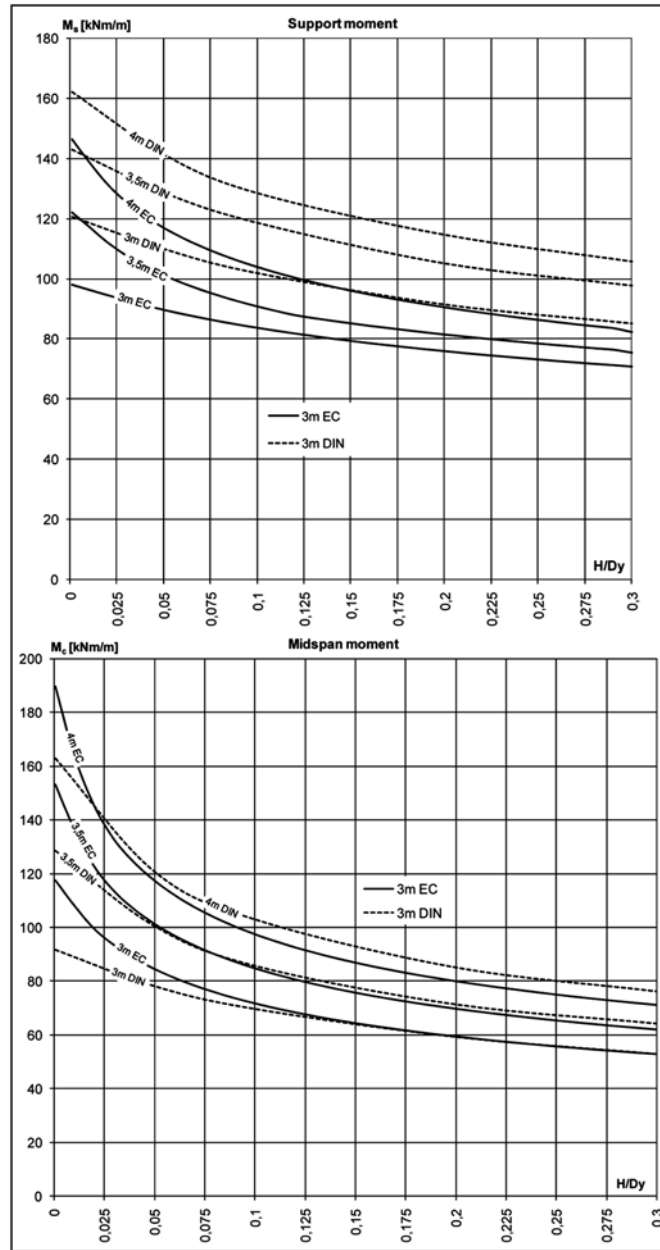


Fig. 18 DIN 1072 and EN 1991-2 comparison of rigid support deck plate moments (one traffic lane)

shown in Fig. 19 (one traffic lane). Comparison between Gauger-Oxford charts (Gauger and Oxford 1983) and new charts is depicted in Fig. 19.

The following conclusions can be made:

1. Hogging support moments are larger for DIN 1072 traffic load, up to spans of 4.5m for both, one and two traffic lanes schemes. This is due to larger axle distance (1.5m) of DIN 1072 SLW vehicle. This vehicle is always going to be positioned above the support when giving the maximum

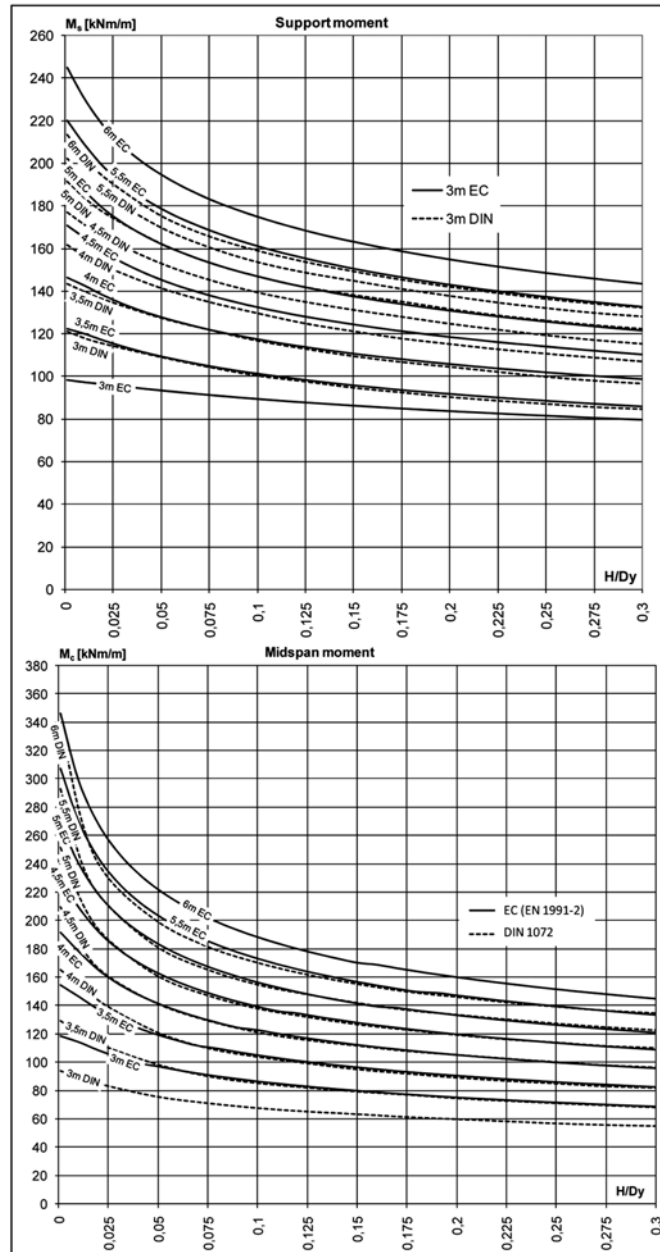


Fig. 19 DIN 1072 and EN 1991-2 comparison of rigid support deck plate moments (two traffic lanes)

hogging support moment. EN 1991-2 vehicle will stay above the support only in case of smaller spans. In these cases, support moments will be smaller due to the smaller axle distance of 1.2m. When positioned in span, EN 1991-2 vehicle will give larger hogging support moments.

2. Mid-span moments are larger for EN 1991-2 but only for two traffic lanes. This indicates that the adjacent vehicle has a larger effect in EN 1991-2, due to the allowed option that the wheels of both

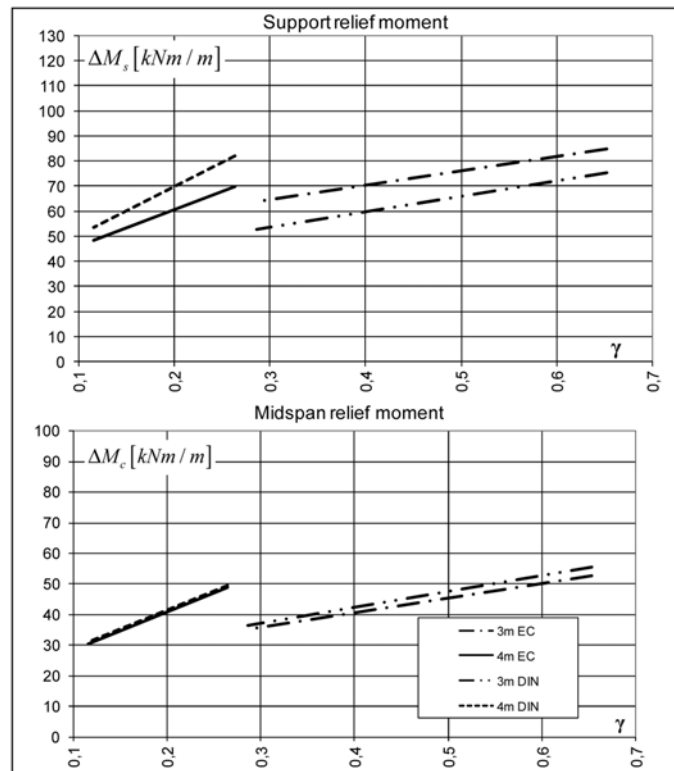


Fig. 20 DIN 1072 and EN 1991-2 comparison of relief moments, one traffic lane

vehicles can be positioned closer, at 0.5m spacing. DIN 1072 vehicles are always at a wheel distance of 1m.

5.2 Relief moments comparison

Diagrams of relief moments are not directly comparable like the rigid support moments are. They do not show the moments directly as readings from two different diagrams are needed, which are then multiplied. Furthermore, to calculate the relief moment, three variables are needed - plate width b , span s , and relief factor γ , so it is not possible to show them as a function in a two dimensional space. Comparisons of relief moments are shown for the same width of 12m so that this variable will be left out. Results for each of the plate are connected by a straight line to better indicate their growth tendency and mutual position. The comparisons of relief moments for one traffic lane are shown in Fig. 20, and for two traffic lanes in Fig. 21.

The following conclusions can be made:

1. Support relief moment is larger for DIN 1072 traffic loads for spans larger than 3.5m. For smaller spans, one of the axles of SLW vehicle will be near the neighboring support and the relative deflection between the two supports will be smaller. This also produces the smaller relief moment.
2. Mid-span relief moment is larger for EN 1991-2 only in case of two traffic lanes. This is due to the larger weight of the heavy vehicle in the second lane (320 kN compared to 300 kN) and its position closer relative to the vehicle in the first lane.

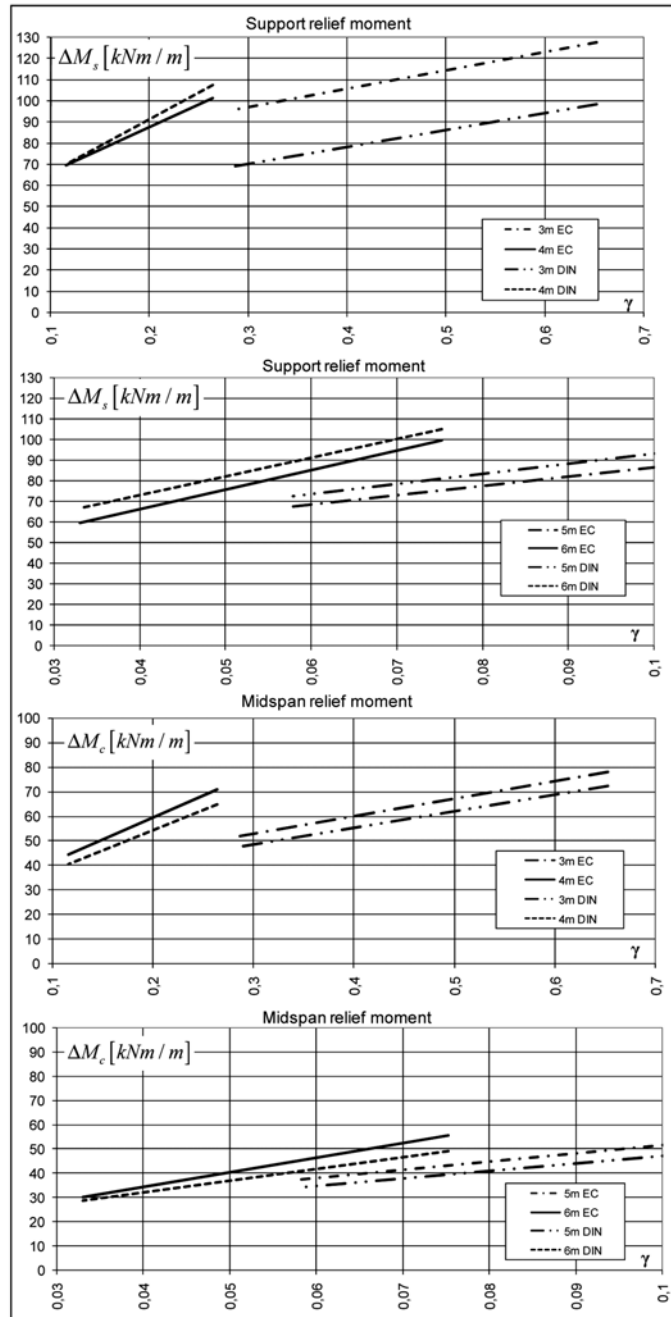


Fig. 21 DIN 1072 and EN 1991-2 comparison of relief moments, two traffic lanes

5.3 Final moments comparison

Tables 2 and 3 show the ratios of the final calculated moments (rigid support moments + relief

Table 2 Mid-span final moments ratios EN 1991-2/ DIN 1072

| $M_{EN\ 1991-2}/M_{DIN\ 1072}$ | s = 3m | s = 4m | s = 5m | s = 6m |
|--------------------------------|-----------|-----------|----------|----------|
| one lane | 1.05-1.15 | 0.95-1.05 | - | - |
| two lanes | 1.15-1.2 | 1.1-1.15 | 1.1-1.15 | 1.05-1.1 |

Table 3 Support final moments ratios EN 1991-2/ DIN 1072

| $M_{EN\ 1991-2}/M_{DIN\ 1072}$ | s = 3m | s = 4m | s = 5m | s = 6m |
|--------------------------------|-------------------------|-----------|-----------|----------|
| one lane | 0.2-0.5 | 0.75-0.85 | - | - |
| two lanes | different sign possible | 0.75-0.85 | 1.05-1.15 | 1.25-1.4 |

Table 4 Support moments ratios EN 1991-2/ DIN 1072 for rigid support deck plate

| $M_{EN\ 1991-2}/M_{DIN\ 1072}$ | s = 3m | s = 4m | s = 5m | s = 6m |
|--------------------------------|-----------|----------|-----------|-----------|
| one lane | 0.75-0.85 | 0.8-0.85 | - | - |
| two lanes | 0.75-0.85 | 0.8-0.9 | 0.95-1.05 | 1.05-1.15 |

moments). Table 4 shows ratios for moments on rigidly supported deck which may be governing for support moment design.

It is necessary to point out that the given Tables are valid for the H/D_y ratios (0.01-0.1) and relief factors γ (0-0.7), which are usual in bridge building. Also, a comment has to be made, that all these moments are shown without partial safety factors (serviceability limit state).

6. Conclusion

By analytical solution of the governing Huber equation, appropriate charts were constructed for fast and simple readings of closed rib orthotropic deck plate bending moments for specific road bridge traffic loads, as specified by EN 1991-2 Load model 1. The calculation procedure is practically the same as Pelikan-Esslinger (Pelikan and Esslinger 1957) and Gauger-Oxford (Gauger and Oxford 1983) procedures, but for the new EN 1991-2 traffic load schemes. Similar diagrams can be produced for traffic loads specified by Load model 3 of any National Annex or for traffic loads from other codes.

References

- EN 1991-2 (2003), *Actions on structures Part 2: Traffic loads on bridges*, September 2003.
- Gauger, H.U. and Oxford, J. (1983), *Erweiterung der Berechnung von Stahlfahrbahnen mit torsionssteifen Längsträgern für die Brückenklasse 60/30*, *Der Stahlbau*, **52**(12), 353-358 (In German).
- Horvatic, D. (1977), *Bridges with orthotropic plates-theory, construction calculation and erection*, Civil Engineering Faculty University of Zagreb, Zagreb 1977.
- Horvatic, D. and Savor, Z. (1998), *Steel bridges*, Croatian Society of Structural Engineers (CSSE), Zagreb 1998.
- Pelikan, W. and Esslinger, M. (1957), *Die Stahlfahrbahn Berechnung und Konstruktion*, MAN-Forschungsheft.
- Troitsky, M.S. (1967), *Orthotropic Bridges Theory and Design*, The James F. Lincoln Arc Welding Foundation, U.S.A., 1967.